# Influence of abradable coating wear mechanical properties on rotor stator interaction

A. Batailly, M. Legrand, C. Pierre

Structural Dynamics and
Vibration Laboratory
–
McGill University

# Outline



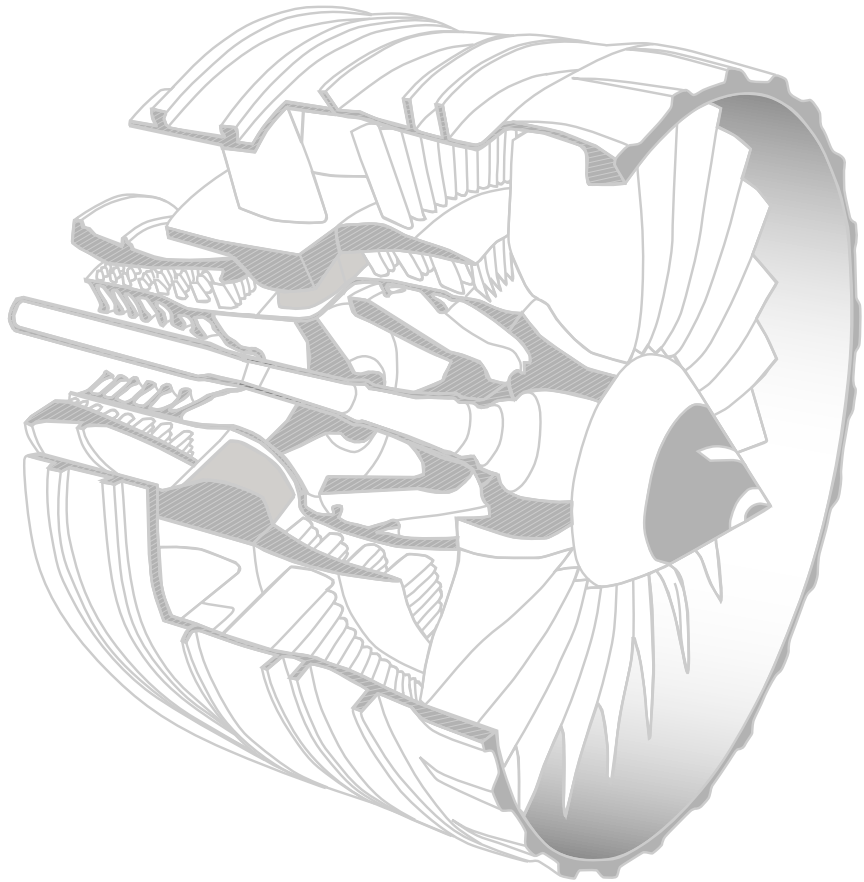

# Industrial context

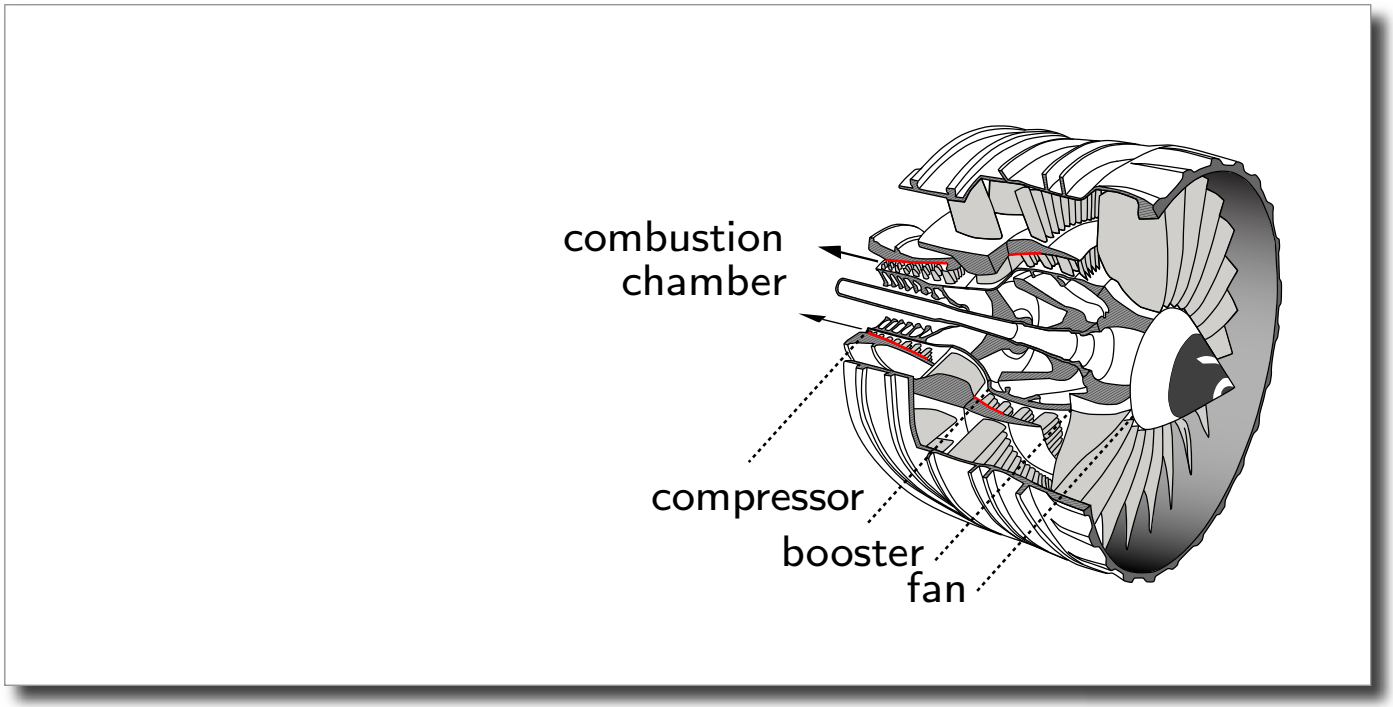


- Modern turbomachines
- Optimization of power efficiency
- $\Rightarrow$ new designs (higher casing conicity, clearance closure...)

# Industrial context

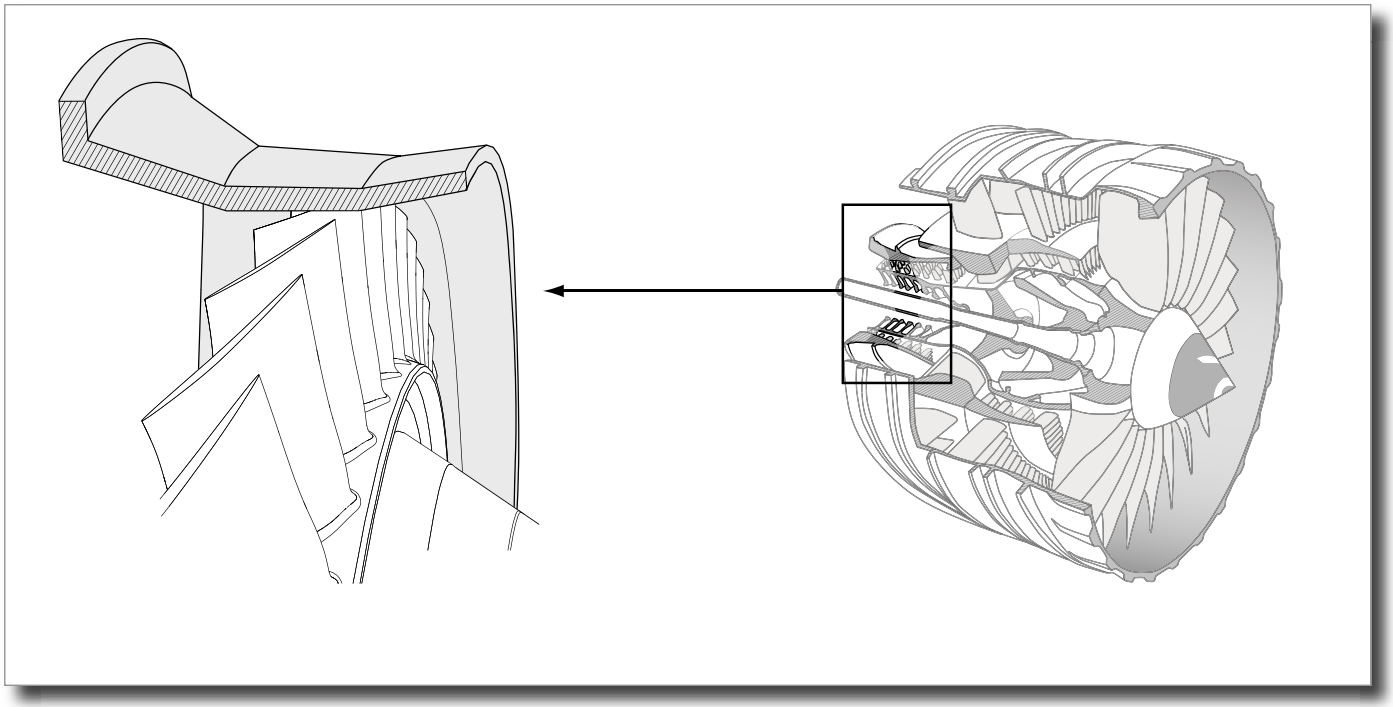

- Compressor stage
- Possible parasitic leakage
- $\Rightarrow$ significant loss of power

# Industrial context

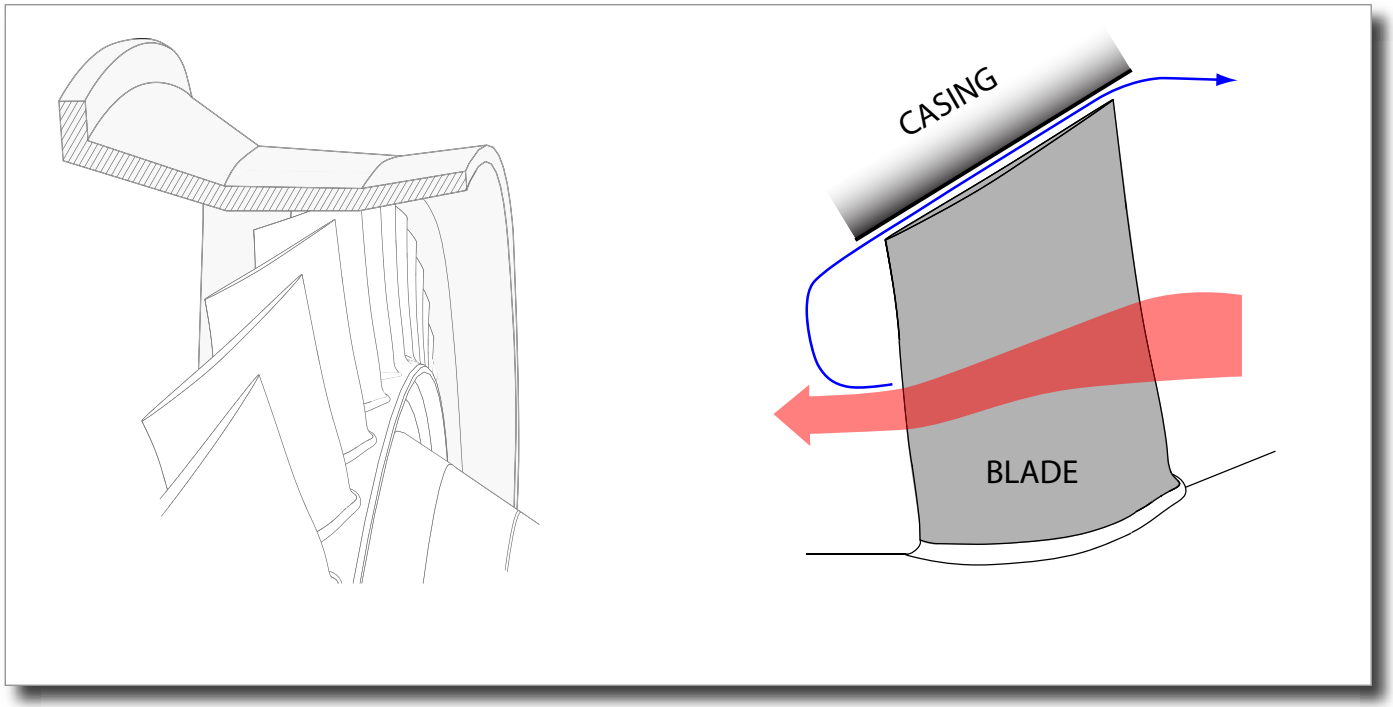


- Compressor stage
- Possible parasitic leakage
- $\Rightarrow$ significant loss of power

# Industrial context

- Modeling of abradable coating
  - Mono-dimensional plastic law
  - Plastic finite-elements around the casing
- Blade / abradable coating contact simulations
  - Variation of the material parameters of the abradable coating
  - Consequences over the blade's amplitude of vibration
  - Consequences in terms of wear level

# Outline



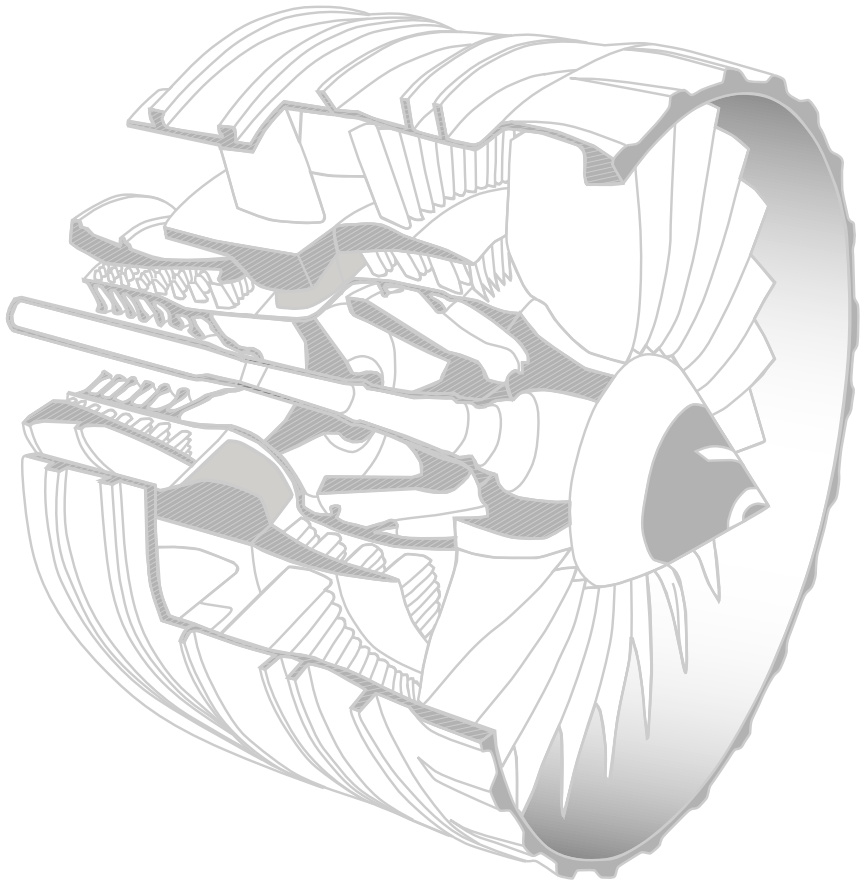

# Blade

- Industrial finite element model ($\simeq$ 65,000 dof)
- 8 nodes used for contact management between the leading edge and the trailing edge
- clamped boundary conditions between the blade and the disk
- use of the Craig-Bampton CMS (ROM contains 85 dof)

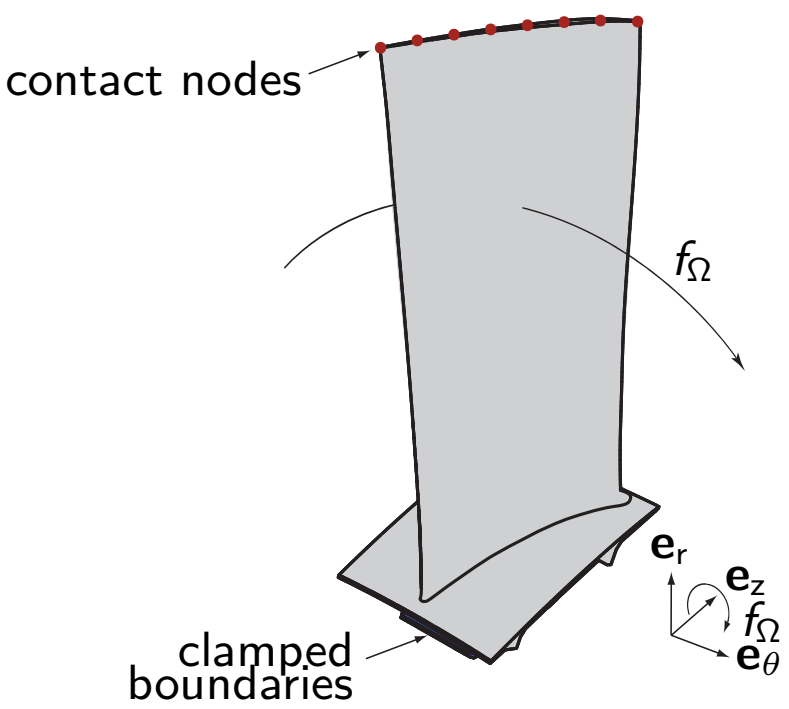


■ *Blade with eight interface nodes*

Both **centrifugal stiffening** and **clearance closure** are taken into account

# Blade

- ROM of 85 dof
- Good approximation of the 8 first eigenfrequencies over the rotational frequency range

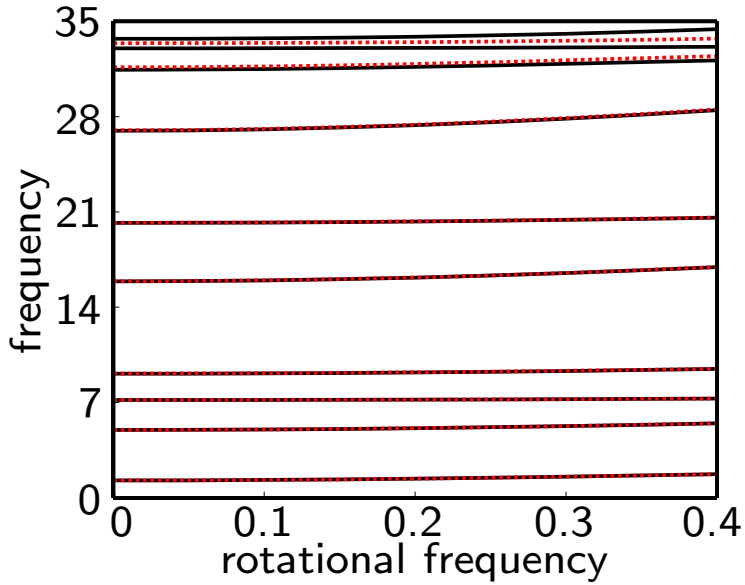


*Campbell diagram of the ROM*

# Outline



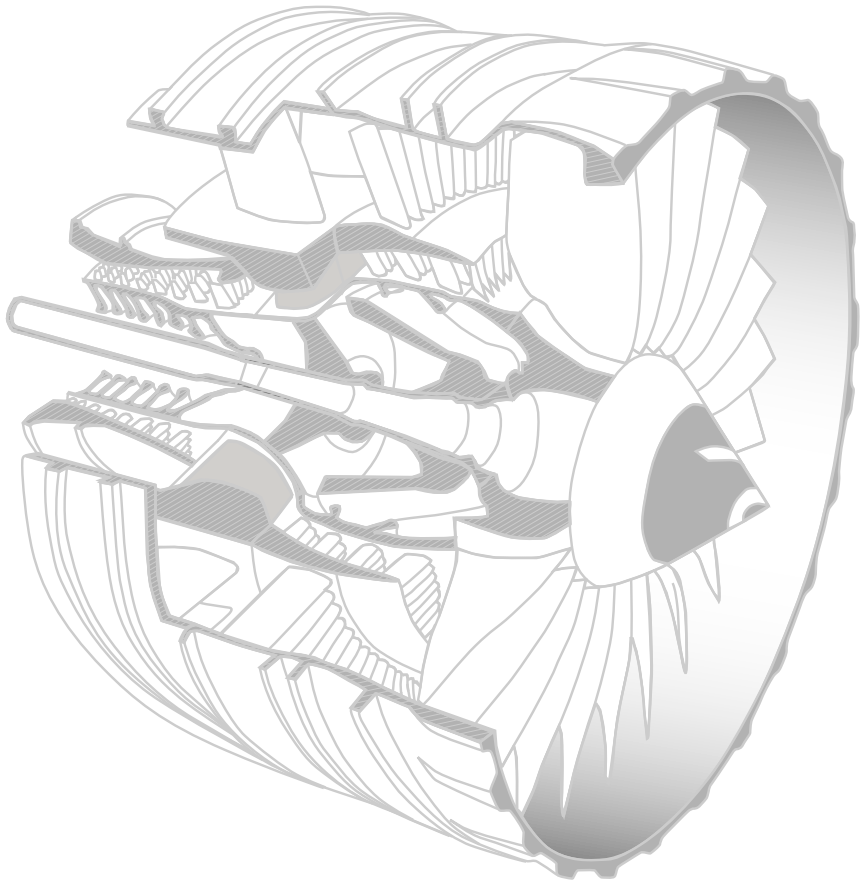

# Contact dynamics

- Master/slave approach (abradable/blade),
- Contact forces computed from plastic deformation of the abradable element,
- Kuhn and Tucker contact conditions: $\forall \mathbf{x} \in \Gamma_c^m$ (master surface)
  $\mathbf{t}_N \geqslant 0,\ \mathbf{g}(\mathbf{x}) \geqslant 0,\ \mathbf{t}_N\, \mathbf{g}(\mathbf{x}) = 0$
  - $\mathbf{t}_N$ discretized contact pressure
  - $\mathbf{g}$ gap function

# Contact dynamics

- Master/slave approach (abradable/blade),
- Contact forces computed from plastic deformation of the abradable element,
- Kuhn and Tucker contact conditions: $\forall \mathbf{x} \in \Gamma_c^m$ (master surface)
  $\mathbf{t}_N \geqslant 0,\ \mathbf{g}(\mathbf{x}) \geqslant 0,\ \mathbf{t}_N\, \mathbf{g}(\mathbf{x}) = 0$
  - $\mathbf{t}_N$ discretized contact pressure
  - $\mathbf{g}$ gap function

Algorithm:

1. **prediction** of the displacements without considering abradable coating,
2. **determination** of the gap function $\mathbf{g}$,
3. **abradable internal forces computation** through a deformation increment $\Delta\varepsilon$ introduced by predicted displacements,
4. **displacements correction** compatible with the calculated contact forces.

# Outline



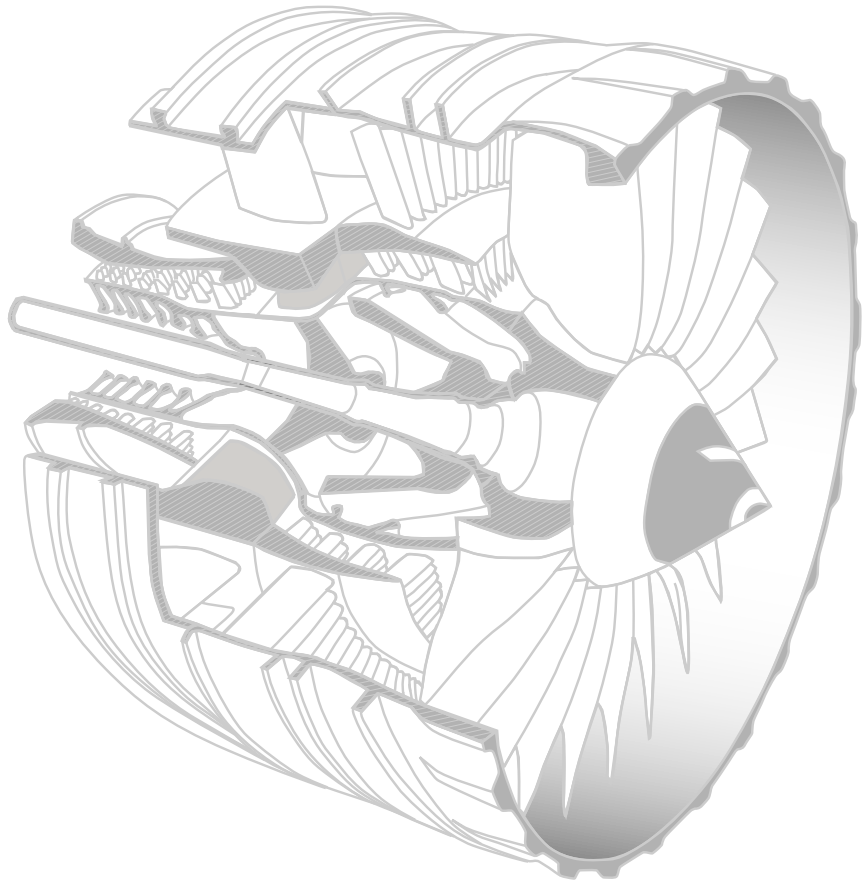

# Theoretical description

- one-dimensional two-node bar elements
- nonlinear plastic constitutive law
- numerical profile in order to represent blade width
- casing is assumed perfectly rigid

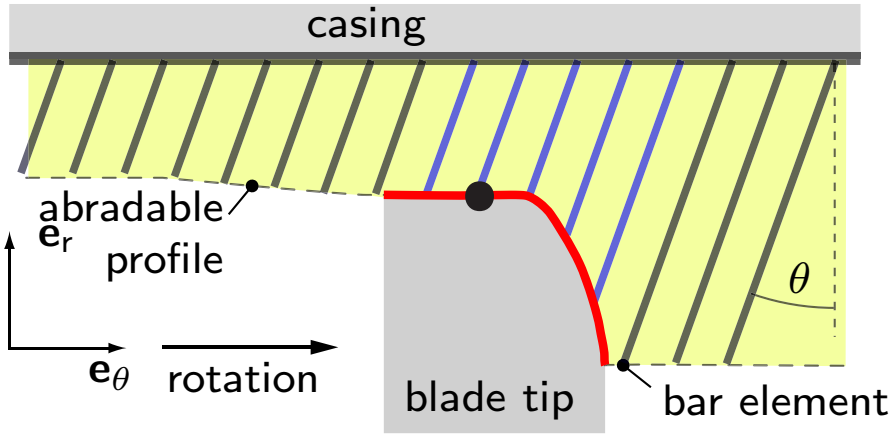


■ *Blade interface node numerical profile*

# Theoretical description

- one-dimensional two-node bar elements
- nonlinear plastic constitutive law
- numerical profile in order to represent blade width
- casing is assumed perfectly rigid

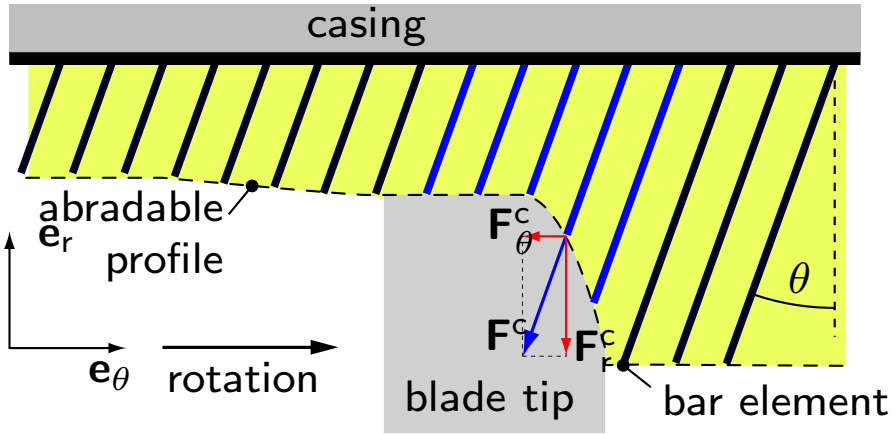


■ *Blade interface node numerical profile*

One layer of abradable elements per contact node on the blade tip

$\Rightarrow$ $\simeq$16.000 abradable elements on the casing

# Theoretical description

Plastic constitutive law

- Young's modulus **E**
- Plastic modulus **K**
- Yield limit $\sigma_Y$

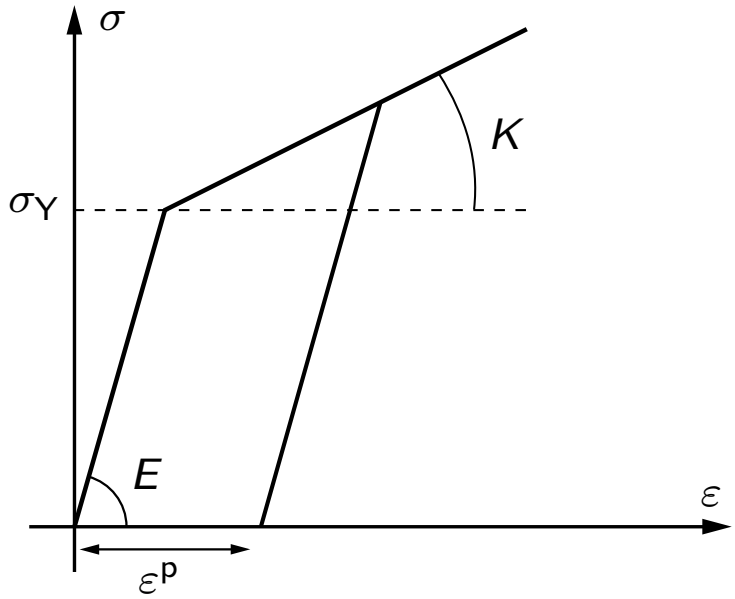


■ *Plastic law for abradable modeling*

# Case study

- Blade-tip/casing abradable interaction,
- One blade (disk dynamics is neglected in this example),
- Imperfections of the casing: deformation along 2 and 5-nodal diameter free vibration modes,
- Simulation parameters (normalized)
  - $\mathbf{E} = 11$
  - $\mathbf{K} = 0.5$
  - $\sigma_Y = 1.5 \cdot 10^{-8}$
  - $f_\Omega \in [0;\ 0.4]$
  - $\theta = 0$

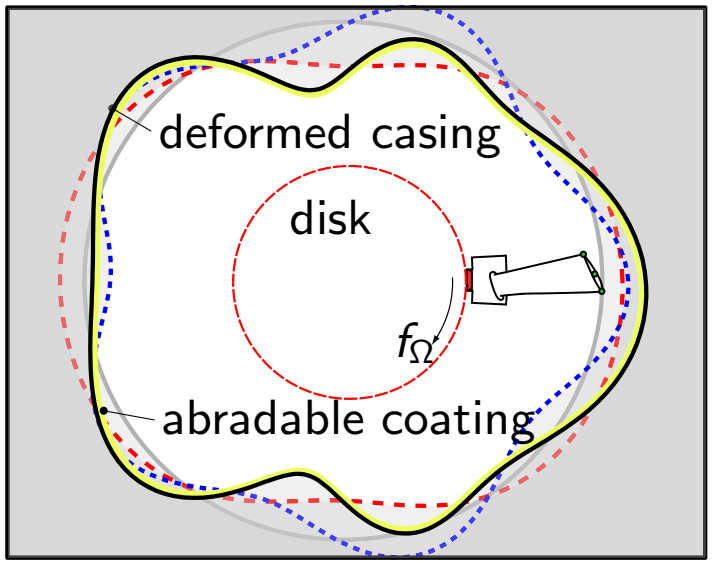


*Casing shapes for case study*

# Case study

$f_\Omega$ dependent wear level map

- Abradable profiles at the end of each simulation pictured with colour code,
- Distinct wear profiles with both odd and even number of lobes,
- Two critical velocities appear.

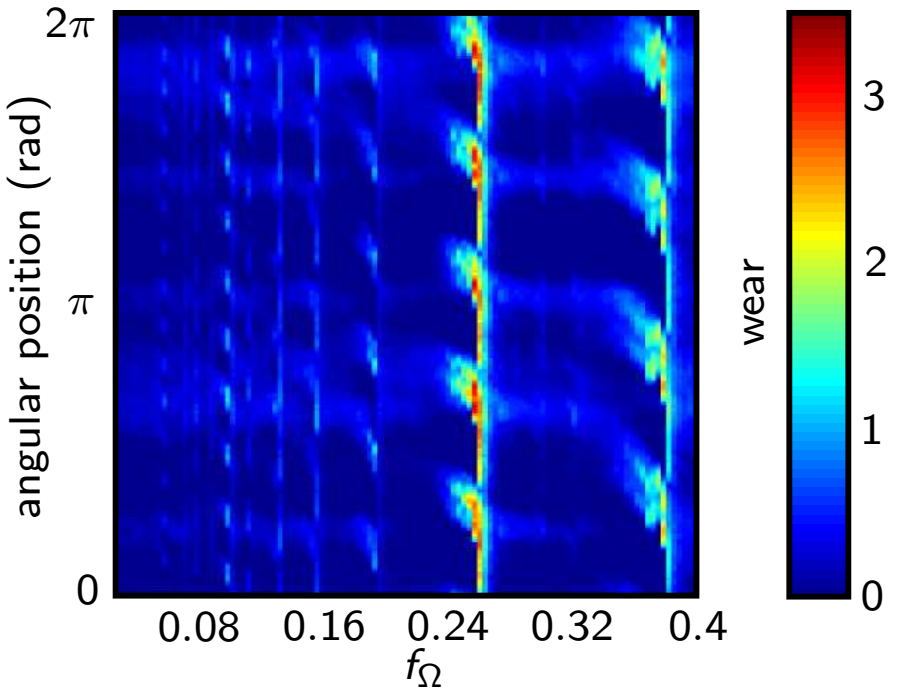


■ *Abradable coating wear patterns*

# Case study

$f_\Omega$ dependent wear level map

- Abradable profiles at the end of each simulation pictured with colour code,
- Distinct wear profiles with both odd and even number of lobes,
- Two critical velocities appear.

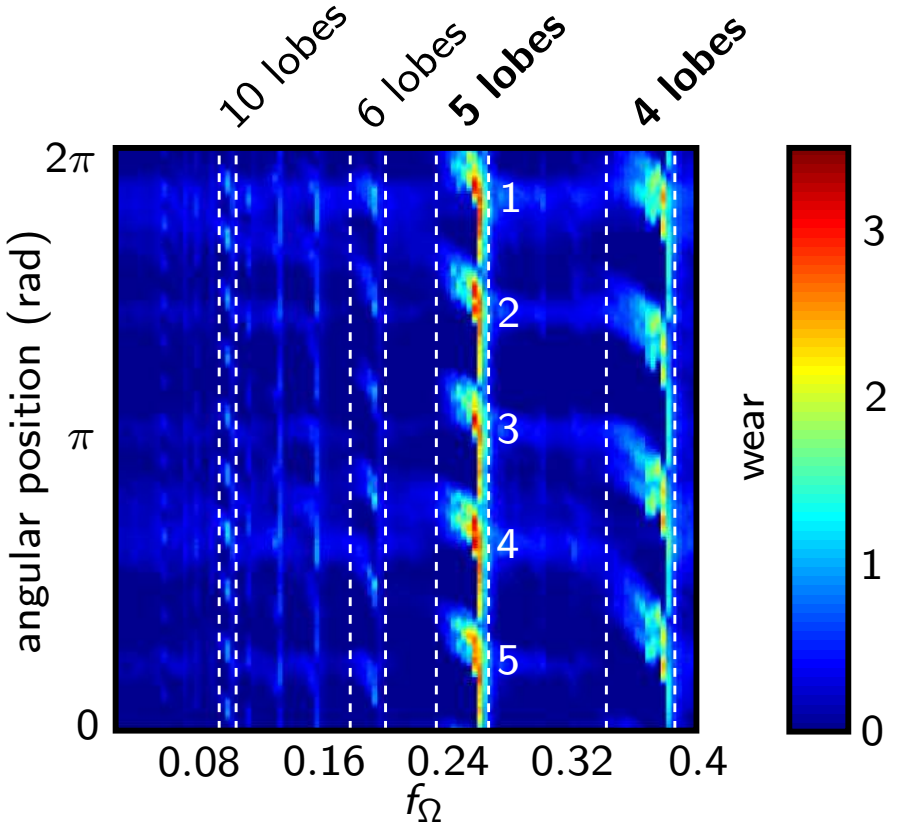


■ *Abradable coating wear patterns*

Complementary results: blade response spectrum for $f_\Omega \in [0;\ 0.4]$

# Case study

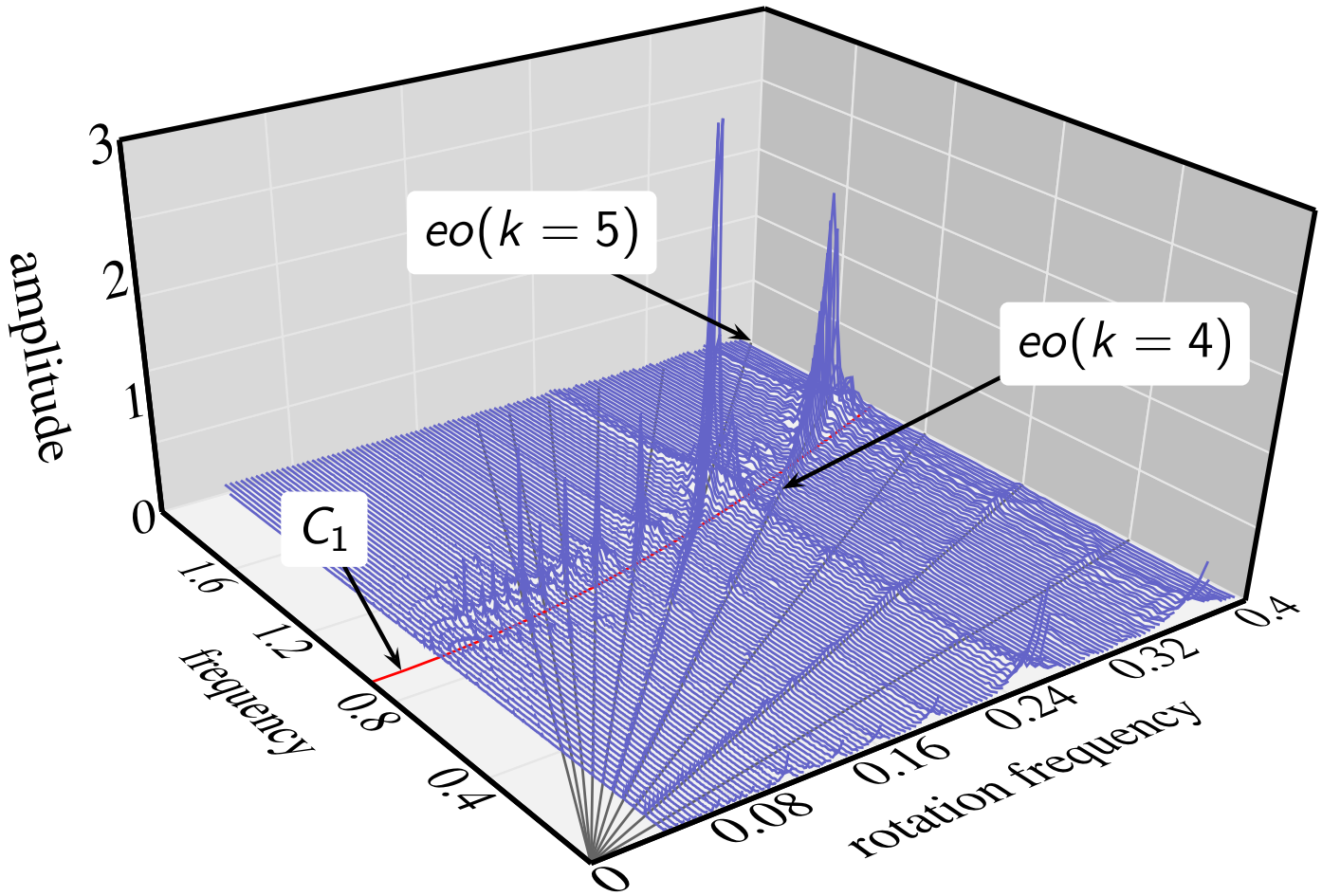


- *Spectrum of the blade response*

# Case study

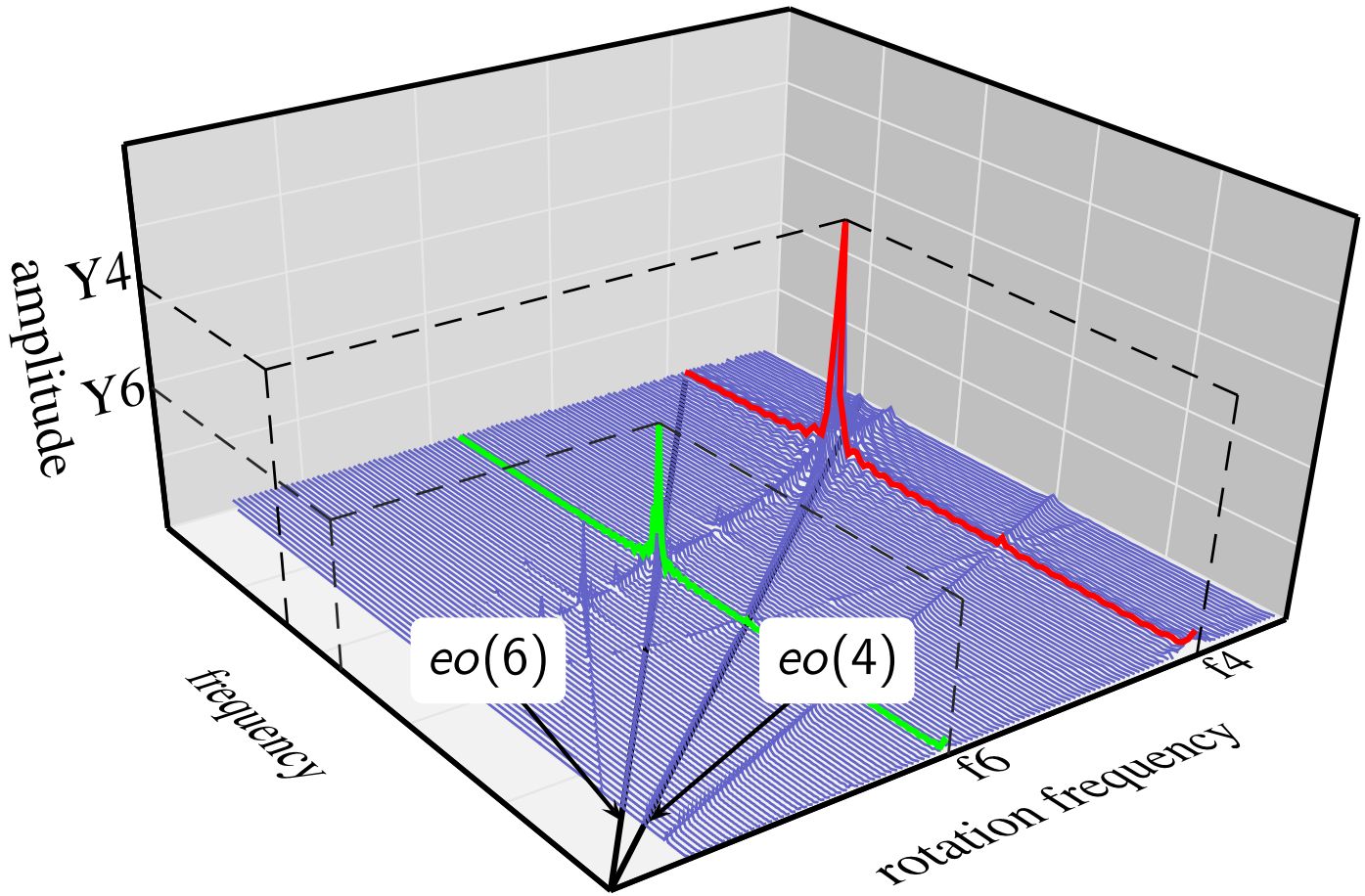


- *Spectrum of the blade response*

# Case study

- Results of this case study highlight potential critical frequencies (located at the intersection of $f_1$ with some engine order lines),
- More simulations may be carried out with different parameters and casing deformed profiles

Most recent results show a good agreement between experiments and simulation

- abradable profile
- blade tip displacements
- critical stress areas within the blade

# Outline



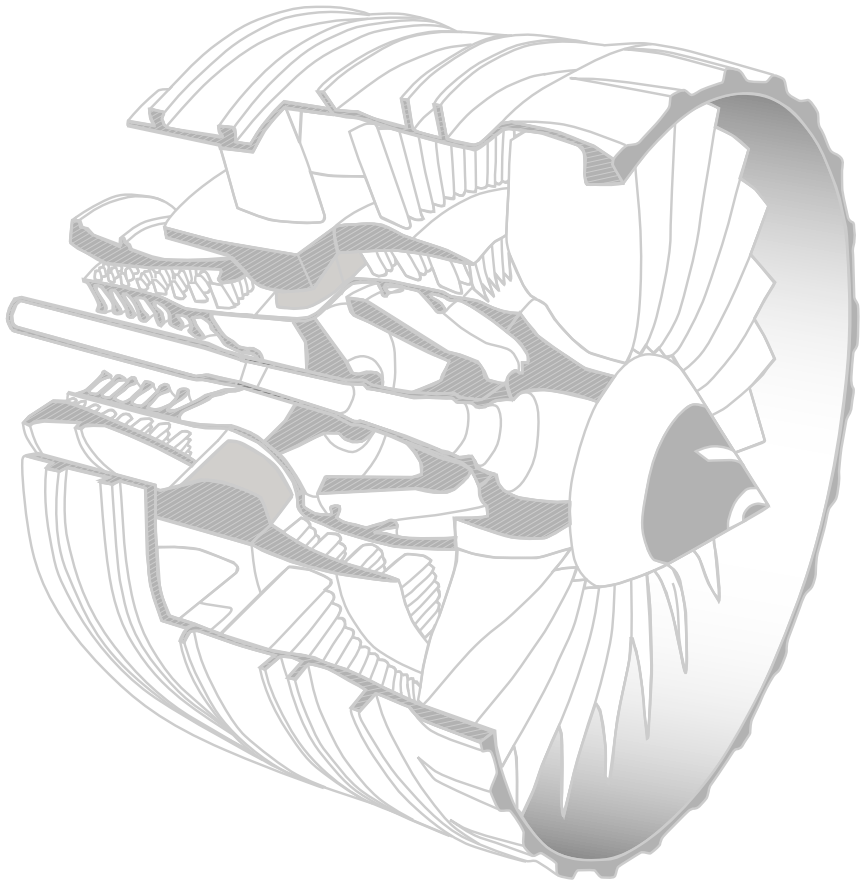

# Material parameters variation

The focus is made on the material properties of the abradable coating (**E**, **K**, and $\theta$)

Large range of values of the Young's modulus between two extreme situations:

1. $\mathbf{E} \to 0$, no interaction, no abradable material
2. $\mathbf{E} \to \infty$, direct blade-tip/casing contact

In total: 9 values of **E** and 5 values of **K** are considered.

# Material parameters variation

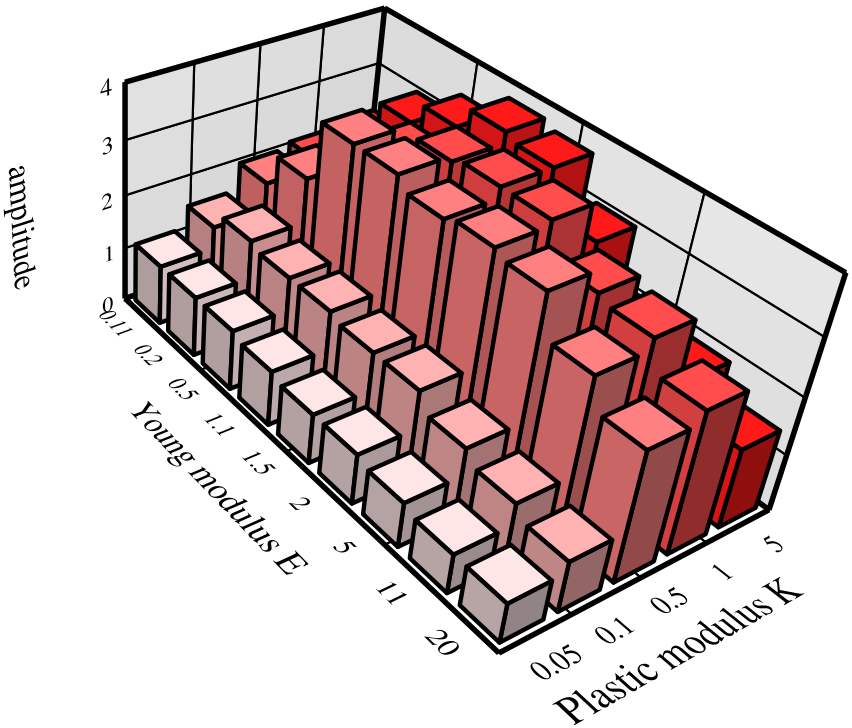


- *Y4 versus E and K*

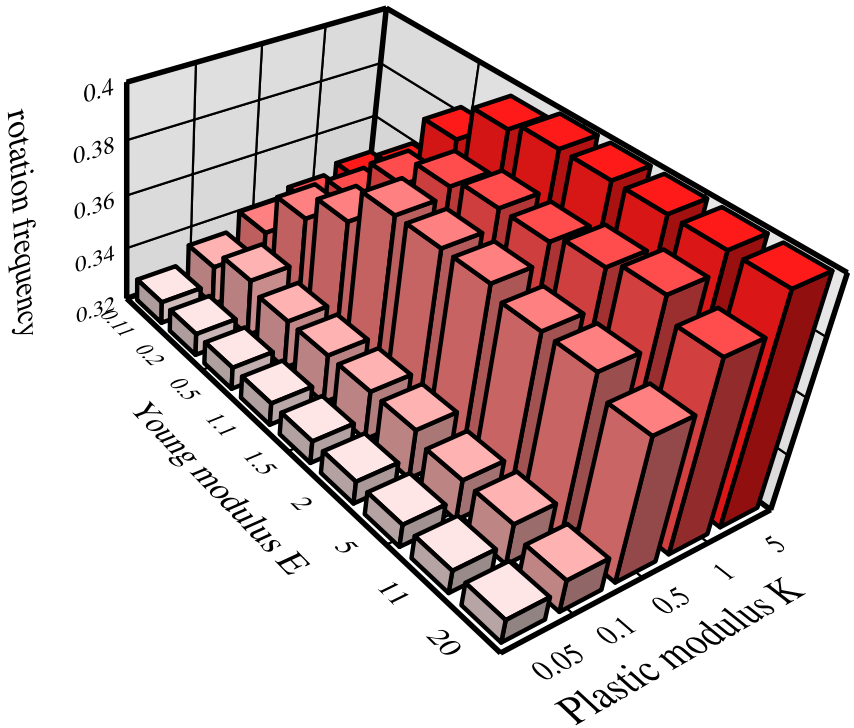


- *f4 versus E and K*

# Material parameters variation

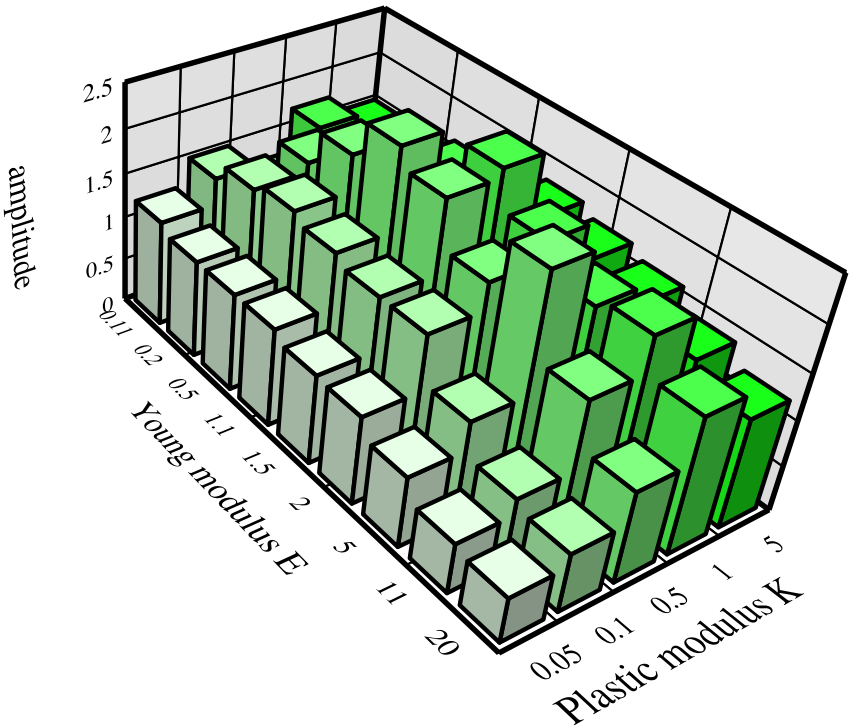


- *Y6 versus E and K*

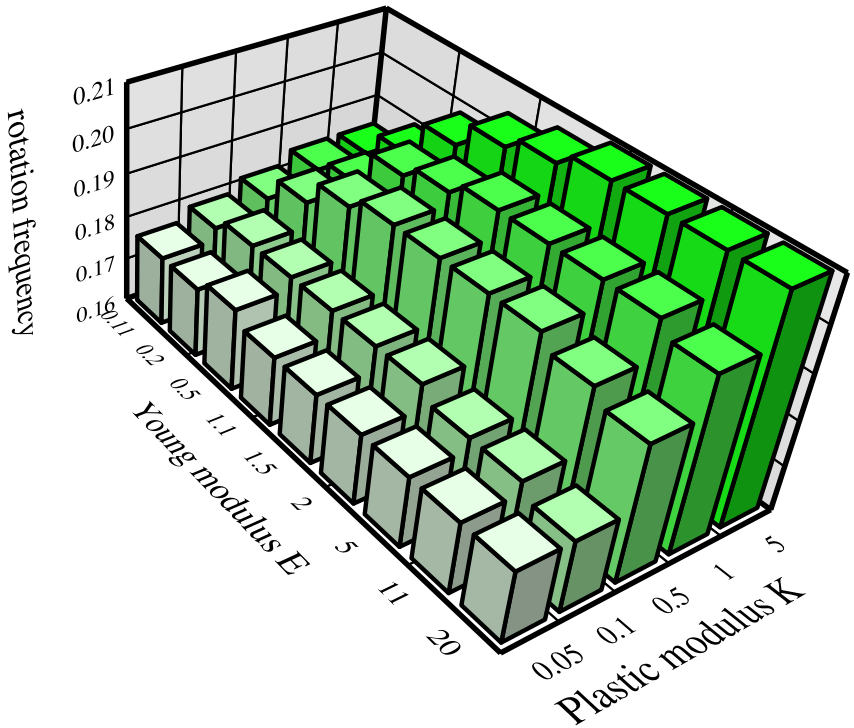


- *f6 versus E and K*

# Material parameters variation

- Results are hardly sensitive to **E** when **K** is small,
- No obvious relationship may be found between the evolution of $Y4$ (or $Y6$) and **E** or **K** $\Rightarrow$ bell-shape evolution,
- A maximum of vibration of amplitude is identified $(\mathbf{E}, \mathbf{K}) = (1.1;\ 0.5)$,

$\Rightarrow$ **Abradable coating may increase vibration level of the blade**

- Contact stiffening phenomenon seems to be essentially dependent on **K**.

# Rotation of abradable elements

- Influence of the $\theta$ parameter controlling the orientation of the abradable elements,
- Contact force has both a radial and a tangential component,
- Investigated values: $\theta = 0$ and $\theta = 0.15$ (usual friction coefficient for blade-tip/abradable coating $\simeq$ 0.15),
- Hypothesis: $\theta > 0$ may lead to more realistic results through the modeling of abradable coating removal force.

# Rotation of abradable elements

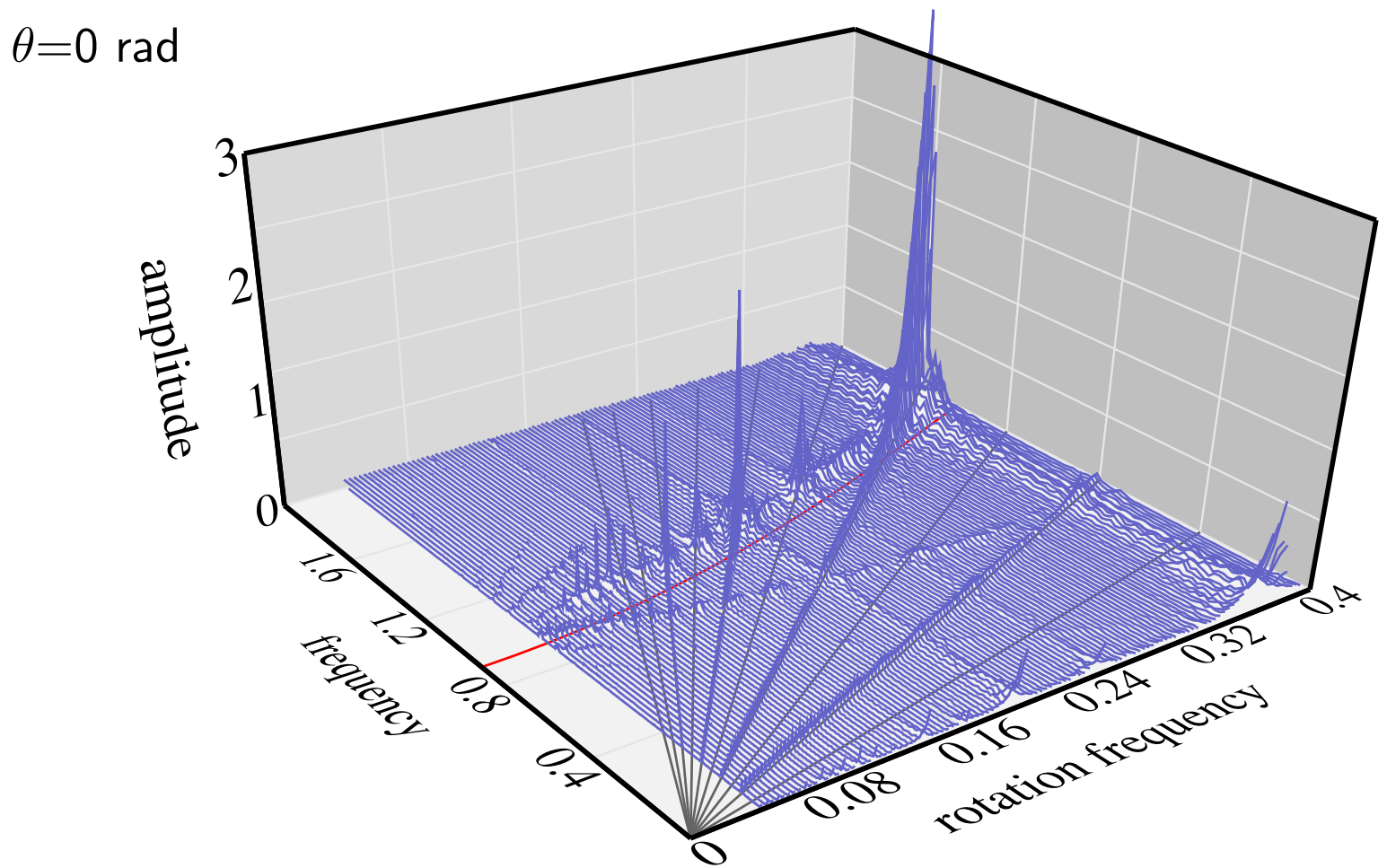


- *Spectrum of the blade response*

# Rotation of abradable elements

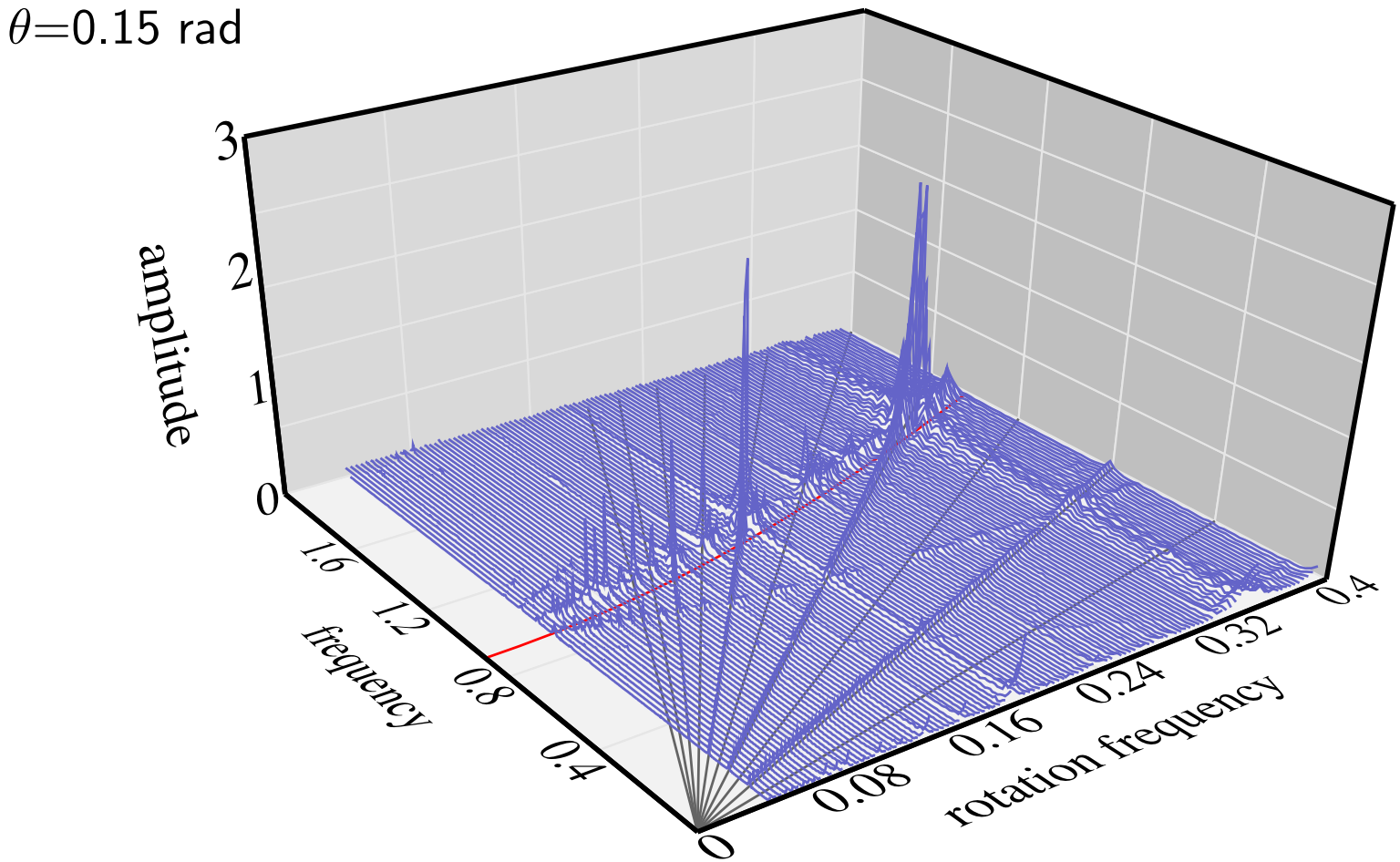


- *Spectrum of the blade response*

# Rotation of abradable elements

- Variation of parameter $\theta$ does not change the nature of the interaction phenomena:
  - first bending mode dominant (design-dependent),
  - similar interaction speed, similar abradable profiles.
- $\theta > 0 \rightarrow$ global softening of the contact case:
  - interaction detected for slightly lower frequencies,
  - amplitudes of vibration decrease.

# Outline



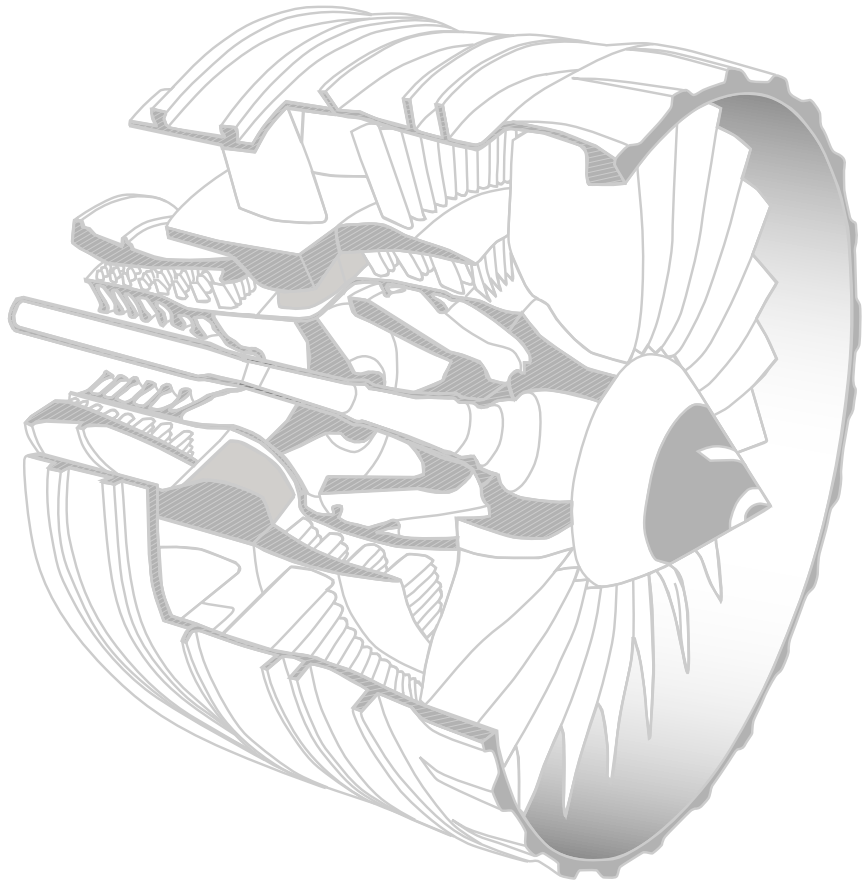

# Conclusion

- Results show that abradable coating mechanical properties strongly influence the interaction phenomena and a maximum of vibration of the blade has been identified,
- The evolution of the abradable coating modeling ($\theta$ parameter) softens the contact case without modifying the nature of the interaction phenomena (number of lobes, interaction speed almost identical),
- The proposed approach seems well suited for an accurate simulation of industrial experiments. Most recent results are encouraging for different types of blades.

# Perspectives

- The proposed strategy may be of great interest for the optimization of blade design:
  - reducing amplitude of vibration,
  - identification of areas where cracks may initiate (maximum stress detection).
- Work is in progress for taking into account the deformation rate $\Rightarrow$ visco-plastic law of abradable coating,
- Calibration of this visco-plastic law will be carried out by direct comparison between numerical simulations and experimental results.

Thank you for your attention.